

Modeling host-seeking behavior of African malaria vector mosquitoes in the presence of long-lasting insecticidal nets



Anna Shcherbacheva^{*,a}, Heikki Haario^a, Gerry F. Killeen^{b,c}

^a LUT School of Engineering Science, Lappeenranta University of Technology, Lappeenranta, Finland

^b Environmental Health and Ecological Sciences Thematic Group, Ifakara Health Institute, Ifakara, Morogoro, United Republic of Tanzania

^c Vector Biology Department, Liverpool School of Tropical Medicine, Pembroke Place, Liverpool, UK

ARTICLE INFO

Keywords:

Malaria control
Mosquito repellents
Long-lasting insecticidal nets
Agent-based modeling
Markov chain Monte Carlo parameter estimation

ABSTRACT

The efficiency of spatial repellents and long-lasting insecticide-treated nets (LLINs) is a key research topic in malaria control. Insecticidal nets reduce the mosquito-human contact rate and simultaneously decrease mosquito populations. However, LLINs demonstrate dissimilar efficiency against different species of malaria mosquitoes. Various factors have been proposed as an explanation, including differences in insecticide-induced mortality, flight characteristics, or persistence of attack. Here we present a discrete agent-based approach that enables the efficiency of LLINs, baited traps and Insecticide Residual Sprays (IRS) to be examined. The model is calibrated with hut-level experimental data to compare the efficiency of protection against two mosquito species: *Anopheles gambiae* and *Anopheles arabiensis*. We show that while such data does not allow an unambiguous identification of the details of how LLINs alter the vector behavior, the model calibrations quantify the overall impact of LLINs for the two different mosquito species. The simulations are generalized to community-scale scenarios that systematically demonstrate the lower efficiency of the LLINs in control of *An. arabiensis* compared to *An. gambiae*.

1. Introduction

The aim of this paper is to present a numerical simulation framework that allows testing various hypotheses concerning the impact of LLINs on malaria vector mosquitoes. Specifically, the work aims to model and determine differences in the behavior between *An. arabiensis* and *An. gambiae* as observed in hut experiments. A population of host-seeking mosquitoes is treated as a number of non-interacting agents driven by external factors. We assume four basic driving effects: the attraction of odor emitted from a host (e.g., CO₂ and sensed by the mosquitoes (see [2,8,9,22,34,37])), repulsion by a physical net barrier, avoidance of a repellent, and the killing effect of the chemicals in the LLIN.

According to data acquired from hut trials in [21], mortality of *An. arabiensis* is consistently lower than that of *An. gambiae* or *An. funestus*. A number of plausible explanations can be offered for the difference in host-seeking behavior of the species. A direct comparison, available from [36], suggests that *An. arabiensis* is a faster feeder than *An. gambiae*, which means that the former spends less time in contact with the skin (or net surface); *An. arabiensis*'s exposure to insecticide treatment is hence shorter, with a lower dosage of chemical consumed. Another

explanation suggests that *An. gambiae* and *An. arabiensis* exhibit different hunting patterns, with a tendency of *An. gambiae* to stay close to the human-baited net (more 'determined' hunting), while *An. arabiensis* exhibits a more random walk near the net. In the model simulation, this would be achieved by more direct movement towards the human. A further alternative explanation suggests that *An. gambiae* and *An. arabiensis* exhibit different levels of persistence in blood-feeding attempts, since odorant receptors of anthropophilic *An. gambiae* are narrowly tuned to compounds of human sweat, see [23,35].

All the above described factors can be implemented in the modeling approach presented here. Each factor needs to be given by a parametric formula, with the parameters calibrated against measurement data, which calls for parsimonious models where the expressions for the basic factors are given with formulas containing a minimal number of parameters.

This work shows how to fit such models to the data of [21]. The identifiability of the parameters is studied using extensive Monte Carlo (MCMC) sampling methods. It is found that the data in [21] does not allow unambiguous identification of all the possible factors, as different model variants are able to give equally good fits. It is demonstrated, however, that all model variants lead to essentially the same results for

* Corresponding author.

E-mail addresses: anna.shcherbacheva@lut.fi (A. Shcherbacheva), heikki.haario@lut.fi (H. Haario), gkilleen@ihi.or.tz (G.F. Killeen).

overall protection efficiency. This finding enables us to model reduced mosquito-human contact rates and increased mosquito mortality in community-scale scenarios consisting of several households with various degrees of protection. The outputs of community-scale simulations demonstrate lower efficiency of LLIN control against *An. arabiensis* than *An. gambiae*, and quantify the higher increase in mortality for *An. gambiae*.

Agent based approaches have previously been applied to model many different aspects of mosquito behavior and malaria transmission. The results of such models highlight, for instance, the role of heterogeneity in host movement, mosquito distribution and density, and the impact of environment on the spread of mosquito-borne disease, [1,4,10,13,24,27]. For instance, in [6] a combination of continuous modeling and agent-based simulation was used to simulate the flight of mosquitoes towards a host in outdoor conditions including wind.

The aim of this work is to characterize the impact of LLINs on host-seeking behavior of different mosquito species. We restrict the model calibration to the situation of mosquitoes and a host in a hut, but the approach can easily be modified for different experimental conditions. Furthermore, the calibrated model can be used to simulate vector dynamics in more complex situations such as, in domains larger in space and time, in combination with continuous modeling as in [6], and with larger host populations with varying levels of protection.

The rest of the paper is organized as follows. In Section 2 we present the modeling approach, the selections and parameterizations for the various factors needed for the modeling, as well as two slightly different approaches to model the difference between the two mosquito species. Section 3 describes the numerical details behind the simulations, and Section 4 gives the results of the model runs. The paper concludes with summary of results and findings, and discussion of further possible applications of the model.

2. Methods

2.1. Mosquito movement and attraction to the host

Our attraction model is based on the assumption that mosquitoes estimate the direction of odor increase (the gradient) by the mechanism of klinotaxis, as is conjectured in [37]. During klinotaxis, a mosquito samples the host odor at one location, then changes location and repeats the sampling, using its memory of the concentration to chose the next position [3,6]. The model in this work aims to comprise essential elements only: movement towards the host, and the effects of the nets and impregnated chemicals on host-seeking and mosquito mortality. While a number of choices has to be made to model these factors, the aim is to develop a parsimonious model with a minimal number of free parameters.

Mimicking the klinotaxis, the flight of mosquitoes is modeled here as a discrete time-stepping random walk. Odour attraction is given by means of an accept-reject procedure: once a random candidate position is selected by the Brownian step, the agent accepts this new position with a probability specified to favor candidate steps towards the attraction i.e., the increased CO₂ concentration, see [25]. The acceptance probability includes the influence of untreated or treated nets and the hut barrier by a rejection function. An untreated net is a physical barrier with close to zero probability of penetration. The model accounts for both for natural mortality and enhanced insecticide-induced death by treated nets, which depends on the accumulated amount of chemical, i.e. the amount of insecticide consumed by the mosquito. At each time step of the simulation, each mosquito is updated individually, with its current condition recorded in a vector of the state (position, accumulation of chemicals, probability of death, etc).

Suppose that at time step $n - 1$ a mosquito-agent is at position \mathbf{x}^{n-1} . The agent randomly selects a new candidate position \mathbf{x}^n by:

$$\mathbf{x}^n = \mathbf{x}^{n-1} + \delta\mathbf{W}, \tag{1}$$

from a 2D proposal distribution. In the experimental runs, the parameters \mathbf{x}_0, σ were matched to imitate the real flight speed of the mosquito, which falls in the range 0.4–1.1 m/s for most species of mosquitoes, as presented in [32]. Thus, the increment $\delta\mathbf{W} \sim N(\mathbf{x}_0, \sigma^2 I)$ was sampled as a random point on a circle centered at \mathbf{x}^{n-1} with radius $R = 0.4$ m with a random number from $N(0, \sigma^2)$ with $\sigma = 0.1$ added in the radial direction.

To reduce the CPU computational time, one simulation step covers 2 s. In the simulations presented, spatial units are given in meters. More detailed models for the flight of insects exist, see [7,17,29,30]; however, the above simple approach is sufficient for the purposes of the present study.

In the absence of any attraction towards a host, the flight of the mosquito is given by the above random walk. Next, we add a mechanism that enables us simulation of movement towards the host in the presence of attraction. Several mechanisms enable mosquitoes to find a human host. Essentially, they are able to sense carbon dioxide (CO₂ exhaled by humans at a long distance and to smell chemical odors emitted from the human body. Many substances associated with human sweat have been identified as attractive for mosquitoes, such as nonanol, lactic acid, ammonia, phenol and many other compounds contained in human sweat [2,8,9,22,34]. Additionally, mosquitoes are able to sense humans at a distance using heat sensors around their mouthparts to detect the warmth of the human body. They are also able to discern movement, colors, shapes and patterns via vision. In general, mosquitoes are unable to recognize the human prey from a distance greater than 80m [3].

As we restrict the model here to the hut experiment situation, the concentration of attractive odor emitted from the individual host is modeled as a solution of the diffusion equation with a point source, which is a Gaussian kernel centered at a spacial position of the host \mathbf{x}^h :

$$C(\mathbf{x}, \mathbf{x}^h) = \exp\left[-\frac{d^2(\mathbf{x}, \mathbf{x}^h)}{2\sigma_a^2}\right], \tag{2}$$

where \mathbf{x} is the position of a mosquito, C stands for a concentration that enables a mosquito to sense the host at a distance $d(\mathbf{x}, \mathbf{x}^h)$. The standard deviation of the Gaussian σ_a determines a maximal distance at which the mosquito is able to sense the host. Naturally, in more complex situations the concentration may be given by other means, such as convection-diffusion models taking into account the spatial geometry, wind, etc [6]. Note that real odor concentrations are not used here, as we scale the concentrations and, moreover, only need the ratios of an attraction potential function as defined below. The movement towards the host is defined as a random accept-reject walk, where the acceptance probabilities are calibrated to fit the measured effects of attractants and repellents.

We employ the main features of the Metropolis algorithm [25]. Suppose that at each point \mathbf{x} we have an attraction potential $p(\mathbf{x})$ that depends on the concentration and other attraction factors. We take a step from point \mathbf{x}^{n-1} to a next candidate point \mathbf{x}^n . If the respective function values are p_{n-1}, p_n , the new point is accepted with the probability:

$$\alpha_n(\mathbf{x}^n|\mathbf{x}^{n-1}) = \min\left(1, \frac{p_n}{p_{n-1}}\right) \tag{3}$$

The CO₂ concentration is regarded as the main attraction factor for mosquitoes. To introduce increasing attraction as approaching the host in a parsimonious way, we simply define the attraction potential as a function:

$$p(\mathbf{x}) = \exp(C(\mathbf{x})/\sigma_{acc}) \tag{4}$$

with a scaling factor σ_{acc} that depends on the distance to the host. A linear distance dependency of σ_{acc} is introduced to account for the vision-activated attraction at a short distance to the host:

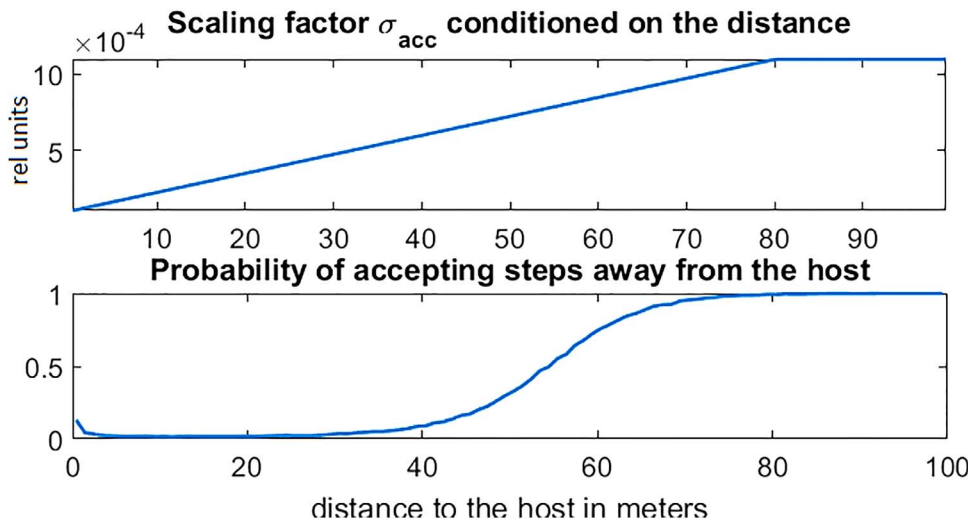


Fig. 1. Scaling factor σ_{acc} conditioned on distance to the host (top), average probability of accepting steps taken away from the host as a function of distance to the host (bottom).

$$\sigma_{acc}(\mathbf{x}) = \begin{cases} \sigma_{acc}^1 + \sigma_{acc}^2 d(\mathbf{x}, \mathbf{x}^h), & d(\mathbf{x}, \mathbf{x}^h) \leq 80 \\ \sigma_{acc}^{\max}, & d(\mathbf{x}, \mathbf{x}^h) > 80 \end{cases} \quad (5)$$

The function increases from the minimum value σ_{acc}^1 with a slope given by the parameter σ_{acc}^2 until it is replaced by a constant. The constant is matched so that the movement is purely random outside the concentration plume. Further details on specifying the constants σ_{acc}^{\max} and σ_{acc}^{\min} are in the next section.

Fig 1 shows the piecewise-linear function for σ_{acc} , as well as the resulting probability of accepting steps away from the host (steps towards the host are always accepted). Note that the parameters of σ_{acc} can be bounded so that the acceptance probability given by (3) is practically 1 at the distance of 80 m from a host, i.e., all moves are then accepted and the movement becomes purely random outside the concentration plume. The next section, Section 3 gives more details of the numerical implementation.

The algorithm essentially mimics the well-known Simulated Annealing optimization method, introduced in [20], but with the ‘annealing temperature schedule’ replaced with a ‘greediness scale’ associated with the distance from the mosquito to the host.

As seen in Fig. 1, the rate of acceptance for steps away from the host decays as the insect approaches the host. In proximity of the host it increases locally but remains quite small. This property can be attributed to a real insect behavior, since in proximity of a host mosquitoes of different species have been observed to exhibit more tortuous flights when scanning the environment before landing [33].

2.2. Modeling treated and untreated nets

Protective devices are modeled using properties of the logistic function:

$$y = \frac{1}{1 + \exp(-x/s)}. \quad (6)$$

The logistic function represents S-shaped behavior of growth. The growth increases exponentially and then slows down for $|x| \rightarrow \infty$.

In order to capture the protective properties of the net, we modify the function so that it attenuates as the distance to the host grows, which parameterized as:

$$\alpha_r(\mathbf{x}|d_{50}, r, s) = r[1 - 1/(1 + \exp(-(d(\mathbf{x}, \mathbf{x}^h) - d_{50})/s))], \quad (7)$$

where $d(\mathbf{x}, \mathbf{x}^h)$ denotes the distance from the mosquito to the protected human (Fig. 2). In our simulations, the above formula gives the probability of rejection at the candidate position \mathbf{x} . The parameters d_{50} and s determine the range of coverage and the spread of the repellent, and r

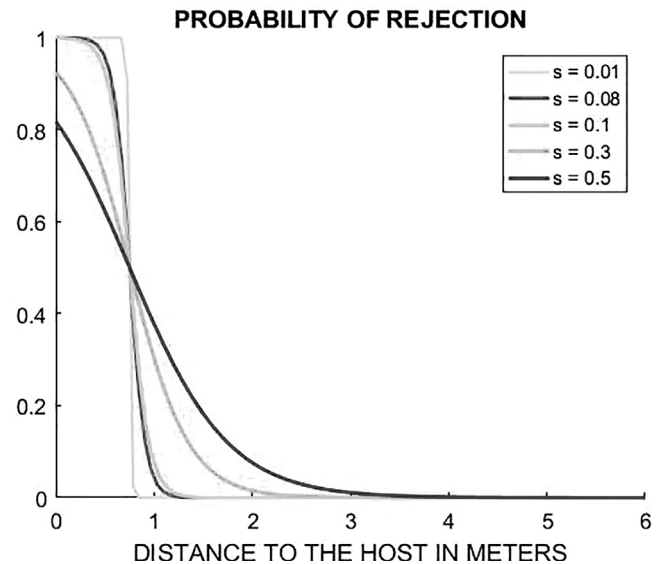


Fig. 2. Probability of rejection associated with repellent for different values of s , with $d_{50} = 0.75$ and $r = 1$.

stands for intensity of repulsion.

Untreated nets. We consider bed nets protecting individuals at night time with fixed actual size comprising 1.5 meters, according to WHO specifications. Untreated nets could be modeled with rejection probability given as a step function, which is a particular case of Eq. (7) when $s \ll 1$. But nets used in rural communities are commonly holed [38]. Hence, deliberately holed nets are used in experimental hut trials (see [21,26]). We simulate torn nets with a penetration probability $1 - p_{net} < 1$ that gives non-zero chance to penetrate the net barrier. So, in the simulations, a proposed step given by formula (1) taken inside the area of the net is accepted with probability $1 - p_{net}$. Estimation results for the parameters of the untreated net case, based on the hut experiment data, are given in the first part of the Results section.

Treated nets. The repulsion by LLIN is computed in two steps. First, we apply the accept/reject step, where the probability of rejection is given by a logistic function describing the chemical repulsion, see Eq. (7). Next, we take into account the physical net barrier just as in the untreated net case. Additionally, LLINs are equipped with the poisoning

effect. When a mosquito consumes the chemical substance spread on the treated net surface, the probability of death increases, which is represented by the insecticide induced mortality.

2.3. Mortality rates

Natural mortality of a population is usually expressed in continuous time, in the form of an ordinary differential equation

$$\frac{dP}{dt} = -\mu P, \tag{8}$$

where the coefficient μ denotes decay rate, and P stands for population number. The connection to discrete-time calculations is easily given by discretizing:

$$\frac{P(t + \Delta t) - P(t)}{\Delta t} = -\mu P(t), \tag{9}$$

where Δt is a time unit. The equation can be written in the form:

$$\frac{P(t + \Delta t)}{P(t)} = 1 - \mu \Delta t, \tag{10}$$

which gives the relative decrease of the population during a time step. Therefore, the probability of death per unit time Δt is computed as the decay rate multiplied by the length of the time interval:

$$\alpha^{\Delta t} = \min\{1, \mu \Delta t\}. \tag{11}$$

In this work we calculate the natural death probability by the above formula with $\Delta t = 2$ seconds, using a literature (see [5]) value for μ that corresponds to 34-hour natural death rates for *An. gambiae* and *An. arabiensis* as 10%.

For each mosquito, the probability of death is tracked separately within the simulation. The probability of poisoning from a unit dosage of chemical is assumed to be the same for *An. gambiae* and *An. arabiensis* [21]. Insecticide-induced mortality rate $\alpha_p^{\Delta t}$ depends on the effective amount of chemical, C_{tot} , consumed by mosquito up to a time instant t . We use here the expression:

$$\alpha_p^{\Delta t}(t) = C_{tot}(t), \tag{12}$$

where the effective amount of chemical consumed by a mosquito is computed as the total accumulated concentration given by the sum of steps in the repellent plume:

$$C_{tot} = \sum_{i=1}^T C^{rep}(\mathbf{x}^i) = \mu_p \sum_{i=1}^T \alpha_r(\mathbf{x}^i | d_{50}, r, s). \tag{13}$$

Here $\alpha_r(\mathbf{x}^i | d_{50}, r, s)$ gives the probability of rejection due to the chemical, as described in Eq. (7). We can interpret the quantity C_{tot} as a scaled chemical concentration with the parameter μ_p scaling the value to the 'effective' poisoning concentration impacting the mosquitoes.

For every mosquito-agent at each step of the algorithm, the total probability of death is computed as the sum of the natural and chemically enhanced probabilities of death:

$$\alpha = \min\{1, \alpha^{\Delta t} + \alpha_p^{\Delta t}\}. \tag{14}$$

Initially, when a mosquito is poison-free, the death rate is restricted to natural mortality. After a mosquito accumulates the chemical, $\alpha = \min\{1, \alpha^{\Delta t} + \alpha_p^{\Delta t}\}$ tends to one, which corresponds a fatal poisoning on taking a lethal dosage of the insecticide.

Remark 1. Note that in Kitau et al. [21] live mosquitoes were collected and kept under glass for 24 h before scoring delayed mortality after the 10 hours in the hut. We imitate the process by fixing the death rate α from Eq. (14) after 10 h in the hut. With α fixed, the probability of death after a 24 h time period is given by Eq. (11) with $\Delta t = 24 \cdot 1800$:

$$\alpha_{24h}^{\Delta t} = \min\{1, \min\{1, \alpha^{\Delta t} + \alpha_p^{\Delta t}\} \Delta t\} \tag{15}$$

Remark 2. In (13) we have postulated a simple functional form for the

impact of the insecticide, which is found to be sufficient for the purposes of the present work. Naturally, more detailed models for the poisoning effect may be employed if such knowledge is available.

Remark 3. The host-seeking behavior, as modeled above by the factors of attraction, is assumed to last only a given maximum time period t_{max} . In the control case without repellents this time is assumed to be 5 h [28]. After t_{max} the mosquito switches to a pure Random walk without influence of the CO₂ concentration. However, the barriers imposed by the net and repellent remain in power, as well as the impact on mortality of the chemicals. Note that we assume that the chemical clue does not impact the movement when mosquito abandons the host-seeking process, either after taking a blood meal sufficient for egg development or after t_{max} spent inside the hut. In our study we assume that sufficient amount of blood is obtained after one feeding on the human host. Additionally, we verified that the resting time after the contact does not impact the overall statistical outcome of the simulations if added in the algorithm, so this feature was excluded for sake of parsimony. In all the simulations we assume that the mosquitoes are not able to interact with each other.

3. Calculation

3.1. Numerical simulations

Details of the numerical simulations are described in this section. In the simulation model, the mosquitoes are represented as a number of agents in a rectangular patch $[x_{min}, x_{max}] \times [y_{min}, y_{max}]$ and are initially considered as having uniformly random spatial positions. For any time point n , we summarize the change of location for every agent from the present position \mathbf{x}^{n-1} as in Algorithm 1.

Several parameters employed in the model are related to given physical factors and hence are fixed for all simulations. Table 1 gives the values used for these parameters.

In addition, it was found that the parameters $\sigma_{acc}^1, \sigma_{acc}^2$ of the function σ_{acc} can be fixed by the following argument. At a distance of roughly 80 m, i.e. outside of the CO₂ plume, the motion is purely random as $C \approx 0$. In the hut experiment this distance is never reached. Moreover, the upper limit for σ_{acc} was selected such that it is large enough to produce Brownian motion outside the plume. Using Eq. (5) and accounting for $\sigma_{acc}^1 < 1$, we find by the requirement:

$$\sigma_{acc}(\mathbf{x} | d(\mathbf{x}, \mathbf{x}^n) = 80) = 0.001 \tag{16}$$

that the second attraction parameter can be given as $\sigma_{acc}^2 = 0.001/80$ (here the numerical value of 0.001 is given by the typical difference values in the concentrations, $\Delta C = C(\mathbf{x}^n, \mathbf{x}^h) - C(\mathbf{x}^{n-1}, \mathbf{x}^h)$, at the distance of 80 m from the host). Given the upper limit, the parameter estimation should identify the value of σ_{acc}^1 , see Eq. (5). However, it was found that the data in [21] only gives an upper bound for σ_{acc}^1 . $\sigma_{acc}^1 = 0.0001$ was selected from the range of possible values.

With these values, the acceptance rate for steps away from the host tends from one to close to zero when the distance $d(\mathbf{x}^n, \mathbf{x}^h)$ decreases from 80 m to zero. This means a gradual transition from random walk outside of the plume to increasingly directional motion at short distances from the host. Fig. 1 illustrates the function σ_{acc} and the resulting average values of the probabilities of accepting steps taken away from the host. At a short distance from the host the acceptance rate for downhill steps exhibits a slight growth. This can be interpreted as a tendency of the mosquito to turn more often before landing on the host [33]. Naturally, more detailed flight data would be required to properly identify the slope of attraction in Fig. 1. However, the present choice is sufficient for the purpose of fitting the data in [21].

Finally, some decisions have to be specified on how to treat the movement at the net, inside the net, on the walls of the hut and at the exit from the hut. If a candidate position gets coordinates inside the net, it is rejected with probability p_{net} , the probability of being blocked by

1. Select candidate position \mathbf{x}^n by adding stochastic increment to previous point, that is compute \mathbf{x}^n by Eq. (1);
2. Account for mortality. Compute the total probability of death by Eq. (14), generate random number $u \sim U[0, 1]$. Remove the agent if $u < \alpha$;
3. Evaluate the concentration of carbon dioxide $C(\mathbf{x}^n)$ at new position \mathbf{x}^n as described in Eq. (2);
4. Compute the scaling factor $\sigma_{acc}(\mathbf{x}^n)$ as given by Eq. (5);
5. Compute probability of acceptance by attraction, $\alpha_a(\mathbf{x}^n|\mathbf{x}^{n-1})$, for position \mathbf{x}^n by Eq. (3);
6. Compute the probability of rejection α_{rej} associated with repellent $\alpha_r(\mathbf{x}^n|d_p, s)$ by Eq. (7);
7. Generate random number $u \sim U[0, 1]$, if $u < \min\{1, \alpha_a(1 - \alpha_r)\}$, mark position \mathbf{x}^n as primary accepted, otherwise, mark position as rejected and remain at the old position $\mathbf{x}^n = \mathbf{x}^{n-1}$;
8. Account for net barrier. If candidate step \mathbf{x}^n is inside and old position \mathbf{x}^{n-1} is outside of the net and position \mathbf{x}^n was primary accepted, generate random number u . If $u < 1 - p_{net}$, accept the new position \mathbf{x}^n . Otherwise, chose closest point on the net \mathbf{x}^{net} to \mathbf{x}^{n-1} and assign new position $\mathbf{x}^n = \mathbf{x}^{net}$;
9. Account for walls. If candidate step \mathbf{x}^n is outside and old position \mathbf{x}^{n-1} is inside of the hut and position \mathbf{x}^n was primary accepted, generate random number u . If $u < p_{hut}$, accept the new position \mathbf{x}^n . Otherwise, chose closest point on the wall \mathbf{x}^{net} to \mathbf{x}^{n-1} and assign new position $\mathbf{x}^n = \mathbf{x}^{net}$;
10. Update the property list of the mosquito;
11. Move to step 1, $n \rightarrow n + 1$.

Algorithm 1. Model algorithm.

Table 1
Fixed parameters.

Parameter symbols	Parameter description	Values	Source
μ_s	average flight speed	0.4 m/s	[32], [33]
σ	standard deviation of the flight speed	0.1 m	[32], [33]
$3\sigma_a$	distance at which mosquito is able to sense a host	80 m	[12]
d_p	size of experimental hut	3 m	[38]
ϵ	width of the net	1.5 m	[38]
t_{max}	minimal distance between mosquito and host treated as an exposure	0.65 m	
s	maximal host-seeking time in absence of chemicals	5 h	[11], [18]
	slope of repellent, characterizes spatial spread of repellent	0.015	[19]

Table 2
Model parameters for the control case and initial guess for the sampler.

Parameter symbols	Parameter description	Value
p_{net}	probability of being blocked by the physical barrier created by the net	0.99967
p_{hut}	probability of exiting the hut	$5.9 \cdot 10^{-4}$

the net barrier. In the case of rejection the mosquito position is updated with the closest point on the net \mathbf{x}^n to the previous position \mathbf{x}^{n-1} such that $d(\mathbf{x}^n, \mathbf{x}^h) = d_p$, where d_p is the net width specified in the Table 2. If the step inside the net is accepted, the direction of the net repulsion is swapped as the mosquito approaches the host under the net. Similarly, if a candidate step gets values outside the hut, it is accepted with probability p_{hut} . In this case we assume that the mosquito enters one of the window traps. Properties and positions of trapped mosquitoes are not updated further, except their mortality status. When a candidate position outside the hut is rejected, we simulate the mosquito hitting the wall. Then the updated position \mathbf{x}^n is selected as the closest point on the wall to the previous position \mathbf{x}^{n-1} . The size of the hut is given in Table 1.

Here, we have only given the steps that impact the movement of the agent. In addition, we have to update a list of properties of each agent by taking into account the accumulated amount of chemical, possible exit from hut, blocking by the net, feeding, switching to random walk, residing inside the net and death. After a mosquito is marked as dead, its position and property list are no longer updated (but the mortality status for a trapped mosquito is still updated at every step).

A mosquito is marked as fed if its updated position is closer than ϵ to the center point of the host, see Table 1. If marked as fed, or if the maximal t_{max} time spent in host-seeking attempts is used, the mosquito switches to a pure random walk (or kinesis), so the accept-reject probability, Eq. (3) due to CO_2 for any candidate position is one. At every next step position Eq. (1) is accepted, unless mosquito hits the net or the wall, or was repelled from the net.

The steps of Algorithm 1 are repeated so that the time period of one night, 10 h, is covered, with the additional delayed mortality taken into account, see Remark 1 in Section 1.3. Thus each calculation simulates a 34 h hut trial. The outcome of the above step depends on random numbers, so the result of each full simulation is stochastic. To calibrate the model against real measurements by estimating the impact of various model parameters, the expected values or averages of the model outputs are needed. This is done by repeated simulations, using many mosquitoes in each simulation. Note that the data in [21] is relative, so

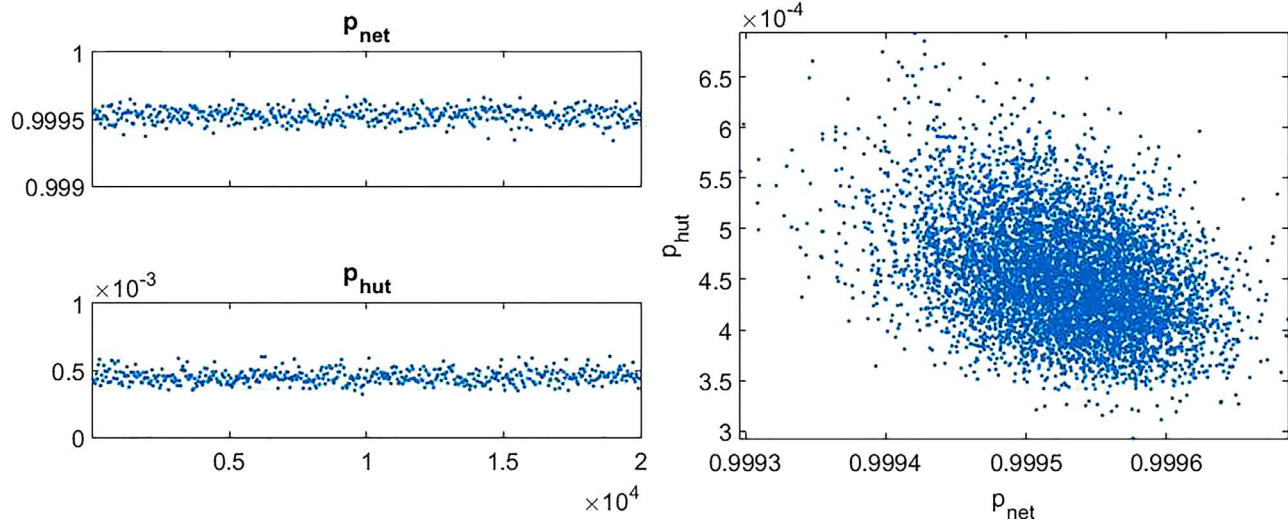


Fig. 3. Parameter chains (left) and pairwise distribution (right) for the control case experiment when the attraction parameters are fixed.

the absolute number of mosquitoes does not impact the calibration.

The repeated simulations for a swarm of mosquitoes are quite CPU intensive. Moreover, to properly study how well the available data is able to identify the model parameters exhaustive computational sampling methods have to be employed. To minimize the CPU times, the computations were carried out by a combination of MATLAB and GPU programming. As each agent can be simulated independently, the calculations are well-suited for parallel computing. To further minimize the computational times, while keeping the model output variances small enough, a compromise between the number of mosquitoes and the number of simulation repetitions was sought. A suitable combination was found to be 6 repeated simulations for a swarm of size 600 mosquitoes. For calculation of the expected values a two-dimensional grid was employed for the GPU runs in which every GPU thread was computed with the above specified algorithm independently. Note that in the LLIN case we compute the cost function twice, corresponding to separate calculation for *An. gambiae* and *An. arabiensis*.

3.2. Parameter identification

The measured values as given in [21] are noisy and with the data uncertainty is given in terms of confidence regions. It is thus natural to ask what is the distribution of all model parameters fitting the data within this noise level of measurements, and to what extent the various model parameters can be identified by the available real data. A common way to answer such questions is via Markov chain Monte Carlo (MCMC) methods. The basic idea underlying MCMC techniques is to sample the candidate parameter points from a predefined proposal distribution and then either accept or reject them according to how closely the model output fits the data. The fundamental technique is the Metropolis algorithm [25]. Here, the use of adaptive methods is especially useful as there is no way to estimate a well-working proposal distribution beforehand. Moreover, to create a reliable sample from the underlying parameter distribution, the number of samples (the length of the MCMC chain), i.e., the number of different parameter combinations tested, must be large enough. For more details see [14–16].

The fit with the data is evaluated via a cost function, a sum of squared residuals of the model outputs O_i and the measurements, M_i :

$$ssum = \sum_{i=1}^{N_f} (O_i - M_i)^2 / \sigma_i^2 \quad (17)$$

Here N_f gives the number of measured responses to be specified separately for the control and treated net cases in the next section. To agree with the confidence intervals of data given in [21] we allow a roughly

30% variation in the model output by setting the measurement error variance σ equal to 10.

The MCMC approach produces a given number of samples, the so called MCMC chain, from the parameter distribution. The main extension compared to traditional least squares parameter estimation producing one 'best fitting' point estimate that minimizes Eq. (17) is that we create 'all' the parameter combinations that fit the measured data within the limits of the confidence intervals estimated for the measurements.

At this point it should be remembered that the model was calibrated for each data set using an adaptive MCMC sampler with chain length 30,000 and each sample consisting of an average of 6 repetitions for an agent swarm of 600 members. The total wall-clock time for such a run, using parallel GPU calculations, was approximately 18 h when performed on a CPU core-i7 2500K, GPU GeForce GTX TITAN.

4. Results

4.1. Control case

As a control case we consider experimental hut trials with an untreated net, modeling the summary outcomes reported by Kitau et al. [21]. It is assumed that *An. gambiae* and *An. arabiensis* exhibit similar host-seeking behavior in the absence of the net treatment, and the same parameters are applicable for both species in the case of these negative controls. The maximum time of a persistent attempt to feed on the detected human host in the absence of any behavior modifying compounds is fixed to 5 h.

In this case two parameters remain to be calibrated: the probability of exiting the hut p_{hut} (as a hedged space) and the probability of being blocked from feeding by the net p_{net} . We fit these against two measured factors ($N_f = 2$) given in [21], namely the exit rate and the percentage of fed mosquitoes for the expression in Eq. (17).

Figs. 3 and 4 present the results of the parameter estimation by the MCMC approach. Fig. 4 shows that the simulated fits of the model against the measurement (the constant line in the figure) are indeed good, and the variability of the model samples matches the given uncertainty of data. Fig. 3 represents the samples of the model parameter distribution that produce the fits. Both separate values for both parameters (the MCMC 'chains') are shown, with the number of samples as the x-axis (left), and the joint 2D distribution (right). The total number of samples was selected as $2 \cdot 10^4$. It can be seen that both parameters are well identified. Moreover, the 2D plot reveals no significant correlation between the parameters.

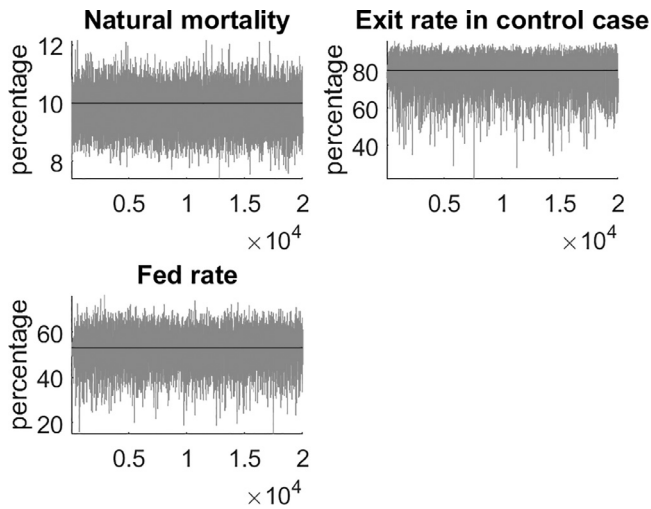


Fig. 4. Model output vs data measurements from [8] for the control case experiment.

4.2. LLIN case

In our simulations the difference in the mosquito species appears only in the presence of the LLIN. As discussed in the Introduction, several options for the difference have been suggested in the literature. We assume that after mosquito spends maximal time t_{\max} hours indoors, it switches to a pure random walk without influence of the CO_2 concentration. As a most simple approach, we first tried the option that only the host seeking time t_{\max}^A of *An. arabiensis* was estimated together with the other LLIN dependent factors d_{50} , s , μ_p , while keeping t_{\max}^G of *An. gambiae* fixed to the same value as in the control case. However, this model variant did not produce a proper fit to the measurements.

Two slightly more complex variants were then studied. In the first version of the model (hence force designated Version 1) the difference between the species is achieved by estimating the host-seeking times t_{\max} separately for each species, while the attraction to the host is kept the same as in the control case. The impact of the LLIN on the mortality is estimated using the same parameter values for both species.

In the second version of the model (henceforth designated Version 2) the host-seeking time in the presence of the LLIN is estimated but kept the same for both species. However, the attraction scaling parameter $\sigma_{acc}^{1,A}$ is estimated for *An. arabiensis* to be larger than in the control case, to capture a lower host-seeking persistence when confronted with the treated net, as suggested in the literature [28].

The parameters for exiting the hut and penetrating the net (see Table 2) are kept the same as in the control case. For the impact of the repellent we employ the function given by Eq. (7), where parameter d_{50} stands for distance from the host when the chemical concentration reaches 50%% of its total.

Next, we compare the factors obtained from our simulations with the corresponding results from [21]. We have six measured responses ($N_f = 6$) available for Eq. (17): exit rates, mortality rates (corrected for control 10%% mortality) and percentage of fed mosquitoes, all separately for *An. gambiae* and *An. arabiensis*. Tables (4) and (5) summarize the parameters estimated, and the mean values of respective Monte Carlo samples. The model outputs versus corresponding data from experimental hut trials for IconMaxx LN reported in [21] are plotted in Figs. 5 and 6. While all of the fits are not ideal, the simulated results are within the error bars of the measurements. Additionally, Table 3 below indicates that both modifications of the model are capable of reproducing the data within the confidence regions.

Next, we discuss the sampled parameter values that produce the above fits of the model to the field data. As in the control case, we show both the separate MCMC chains for each parameter and pairwise 2D distributions. Note that since the chemical used (IconMaxx LN) is short-

range, we can postulate that the repelling distance is less than 10cm, and fix accordingly the value of the parameter s that determines the range of the effect. Fig. 7 gives the separate parameter chains for Version 1 of the model for the remaining parameters d_{50} , r , μ_p , t_{\max}^A , t_{\max}^G . It can be seen that all the parameters are bounded both from below and from above, but relatively large variances remain. A more detailed view is given by Fig. 8, which shows the pairwise scatter plots of the parameters. In particular, the 2D distribution of the values of t_{\max}^A and t_{\max}^G should be noted. The distribution shows a clear correlation between the values; the host-seeking time of *An. gambiae* is consistently larger, roughly two times that of *An. arabiensis*. Moreover, for both species the estimated values are clearly lower than that used in the control case (5 h). It may be concluded that while the data restrict the parameter values and can reveal some logical correlations between them, the data are not able to accurately identify parameter values. Parameter chains and pairwise parameter distributions for Version 2 are given in Figs. 9 and 10. Again, the parameter values are bounded from below and above, but clear correlations remain, as well as relatively large uncertainties for several parameters.

It can be concluded that the hut-level data used in this study only partly restricts the model parameters, and rather different values of short-range attraction or host-seeking times in the presence of the LLINs are able fit the data within the reported error limits. However, the overall impact of the LLINs, which differs for the two mosquito species considered, is captured by the model, as shown in the next section.

4.3. Community scale simulations

In spite of the large uncertainty in the parameter distributions the model can be used to quantify the overall impact of the LLINs: the different model versions, simulated using randomly selected parameter values from the MCMC chains, continue to produce essentially the same results when extrapolated the simulations from the hut level to the community scale, i.e., to situations containing several households and hosts with various degrees of protection by nets and chemicals. In this setting it is observed that the LLINs are systematically less efficient at controlling *An. arabiensis* than *An. gambiae*.

To demonstrate the reduced efficiency of LLINs at controlling *An. arabiensis* a community level example is simulated with the two modifications of the model as given in the previous section. For the simulation example 20 persons are positioned in 4 households of the same size, 5 people in each household. The households are located at a distance of no less than 10 m from one another. All the results were averaged over three simulation repetitions for both model variants, using different parameter vectors randomly selected from the parameter posteriors presented in Fig. 9. The time period for the simulations was again one night, from 6 pm to 6 am. While in the hut level experiment mosquitoes can only exit from the hut into the window traps, in the community level experiment we assume realistic village conditions, where mosquitoes are able to move between huts. Note that we only discuss the results of this one example here, but consistently similar results were obtained for a large variety of settings of households and people.

To estimate the impact of the LLINs simulations were performed with increasing levels of LLIN coverage of the hosts, with the percentage of protected individuals varying from 10%% to 100%%. In this way, respective increasing and decreasing values for mosquito mortality and mosquito-human contact rates were obtained as shown in Fig. 11. Moreover, the reproductive number can be computed, defined as the number of secondary cases (infections, see [31]):

$$R_0 = ma^2bce^{(-gn)}/g. \quad (18)$$

Here g is the death rate of mosquitoes, a stands for mosquito-human contact rate, m denotes the number of female mosquitoes per human, η is the number of days required for sporogony (commonly 10 days for most of species of mosquitoes), b is the probability of transmission of

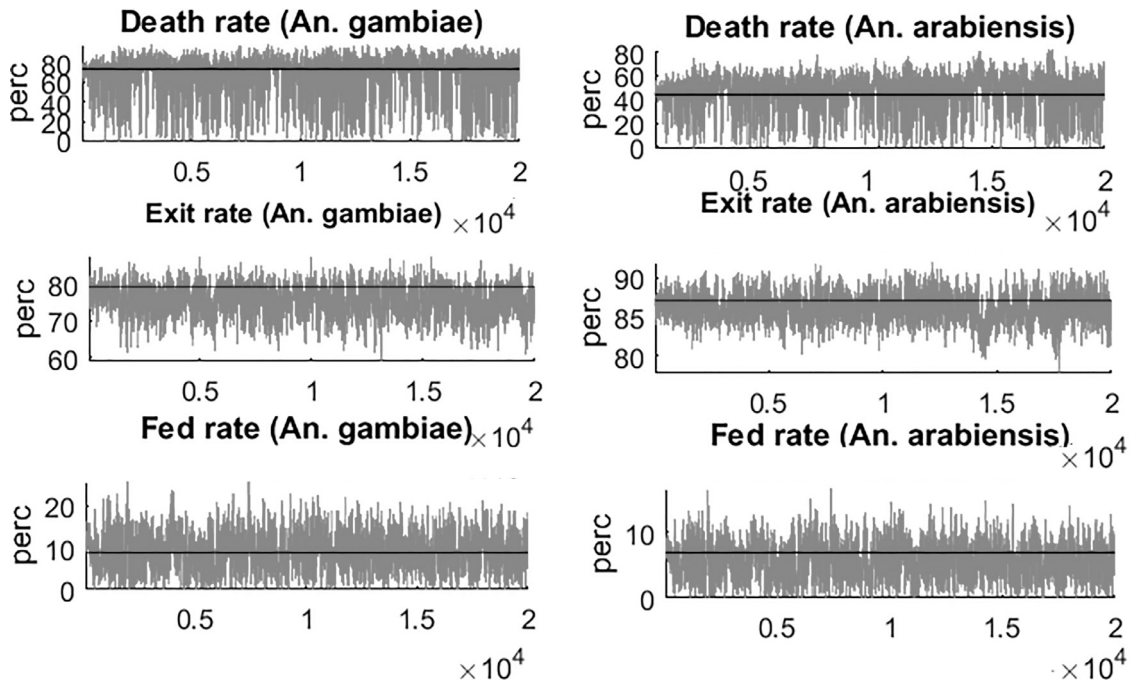


Fig. 5. Sampled cost function values of Version 1 versus field observations in [21]. The LLIN is treated with IconMaxx LN treatment kit.

sporozoite from an infected mosquito to a susceptible human, and c gives the probability of transmission of the sporozoite from infected human to mosquito. As we are interested in the relative decrease of R_0 we can set $m = b = c = 1$. The nonlinear factors of R_0 , the daily mosquito mortality g and the mosquito-human contact rate a are given by the averaged results of the simulations.

While the simulation results are stochastic, a clear decreasing trend of R_0 as a function of the protection can be seen from Fig. 11. Moreover, the variability within the model versions is of the same order as the variability between the versions. Thus, we can conclude that both model versions produce statistically identical results for the average

Table 3

Model outputs for versions 1 and 2 (V1 and V2, respectively) versus field observations reported in [21]. The LLIN is treated with IconMaxx LN treatment kit.

Source	An. gambiae			An. arabiensis		
	V1	V2	[21]	V1	V2	[21]
death	72	72	74 (59–89)	46	48	45 (37–51)
exit	77	77	79 (62–89)	88	82	87 (77–92)
fed	10	10	9 (2–34)	7	5	7 (2–21)

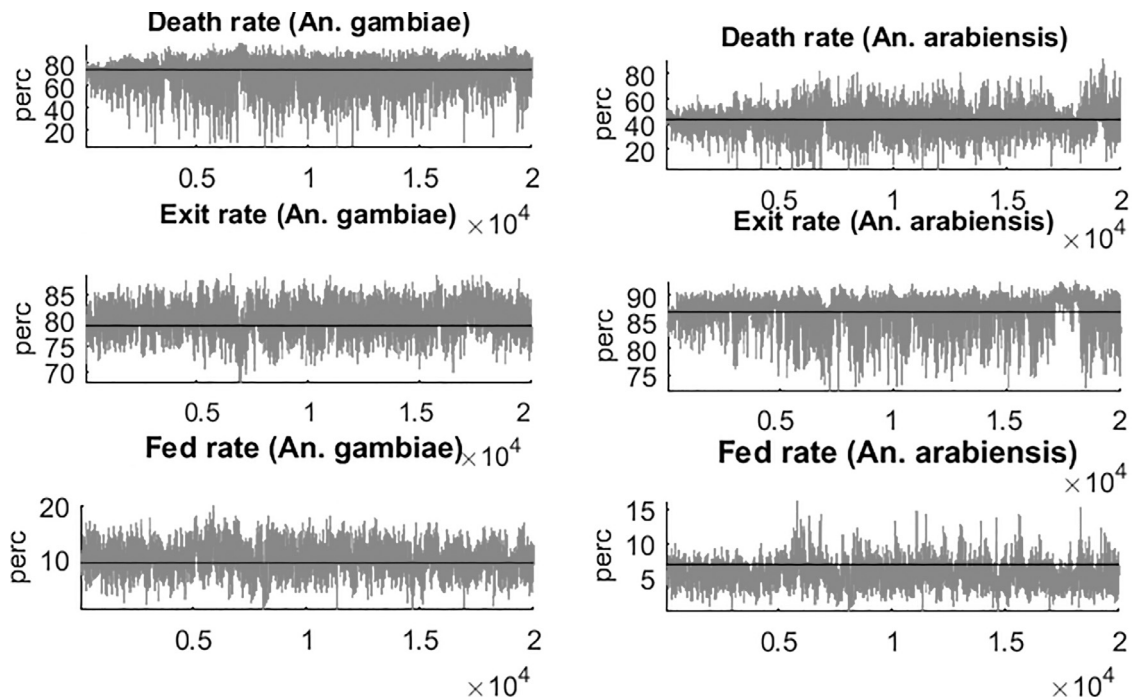


Fig. 6. Sampled cost function values of Version 2 versus field observations in [21]. The LLIN is treated with IconMaxx LN treatment kit.

Table 4
Model parameters for the LLIN and mean values of the sampled parameter chains (Version 1).

Parameter symbols	Parameter	Values
d_{50}	range of repellent coverage	0.755
μ_p	insecticide-induced death rate	$4.4 \cdot 10^{-8}$
r	intensity of repulsion	0.88
t_{\max}^A	maximum host-seeking time for <i>An. arabiensis</i>	1.2 h
t_{\max}^G	maximum host-seeking time for <i>An. gambiae</i>	4.0 h

Table 5
Model parameters for the LLIN and mean values of the sampled parameter chains (Version 2).

Parameter symbols	Parameter	Values
d_{50}	range of repellent coverage	0.755
μ_p	insecticide-induced death rate	$4.4 \cdot 10^{-8}$
r	intensity of repulsion	0.88
t_{\max}^{LLIN}	maximum host-seeking time for both species	4.0 h
$\sigma_{acc}^{1,A}$	minimal value for the scaling factor (<i>An. arabiensis</i>)	$7 \cdot 10^{-4}$

impact of the LLINs in a community level setting, even if the detailed mechanisms of the impact of LLINs on short-range mosquito behavior are not fully identified.

Although the contact rates are similar for both species, the results reveal systematically lower mortality rates for *An. arabiensis* than *An.*

gambiae, which implies lower efficiency of LLINs in control of the former mosquito species. Comparing the reproduction numbers R_0 for different LLIN coverage, it was observed that the minimum coverage guaranteeing disease eradication is higher for *An. arabiensis*.

5. Discussion

We presented an agent-based approach to model the attraction of mosquitoes towards a human host and calibrate the model with the field data extracted from [21]. Several model variants were tested to arrive at the most parsimonious version that contains the basic factors: the movement towards host, the effects of the net and chemicals, and mortality.

Initially, the control case of mosquito host-seeking in the presence of an untreated bed net was simulated for *An. gambiae* and *An. arabiensis*. Here no difference between *An. gambiae* and *An. arabiensis* was assumed: the same host-seeking time was used for both mosquitoes, and similar sensitivity to a host was assumed. Next, the host-seeking in the presence of the LLIN was modeled. Different model parameterization versions were selected to test various hypotheses explaining the different host-seeking behavior of the species. In the first version of the model maximum hosts-seeking time was estimated separately for both species to achieve closer correspondence with the data. In the second version the same host-seeking time was used for both species and a minimum scaling factor was estimated for attraction of *An. arabiensis* that reflects reduced host-seeking persistence when confronted with the LLIN. In both modifications the same values for insecticide-attributable incremental mortality and deterrence parameters were assumed for both mosquito species. Possible model parameter values were sampled by using extensive MCMC simulations. It was found that the available data does not allow unanimous discrimination of all such optional factors. However, certain trends could be extracted from the parameter posterior distributions. For instance, regardless of the other covariate values *An. arabiensis* was estimated to consistently abandon blood feeding attempts much earlier than *An. gambiae* when confronted with the treated net.

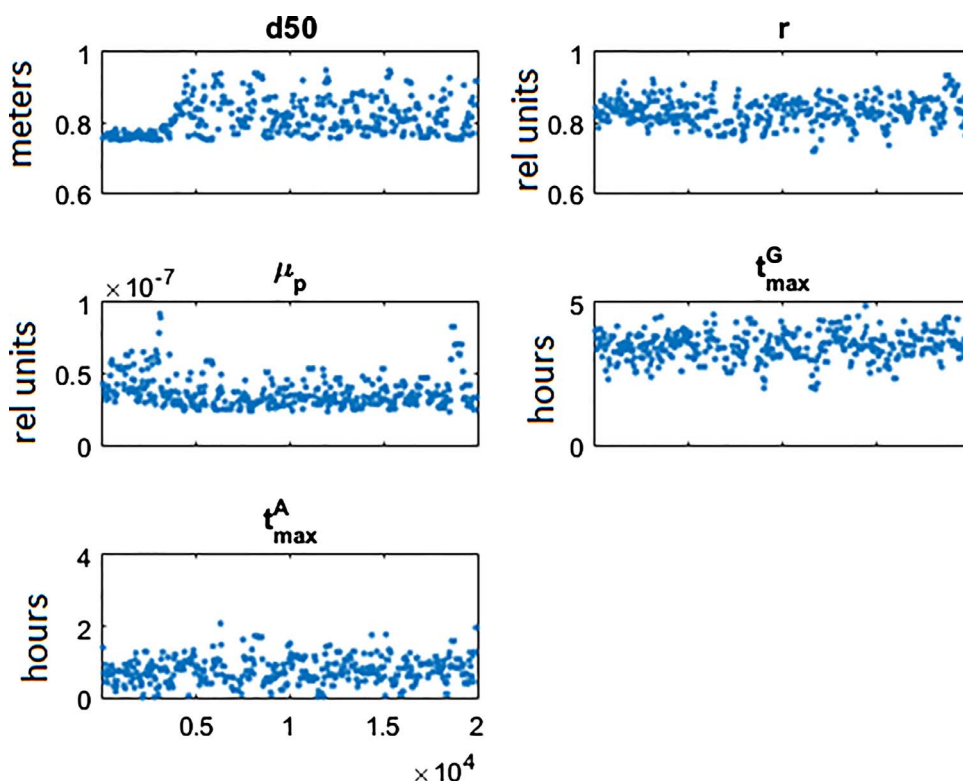


Fig. 7. Parameter chains for Version 1 for LLIN treated with an IconMaxx LN kit.

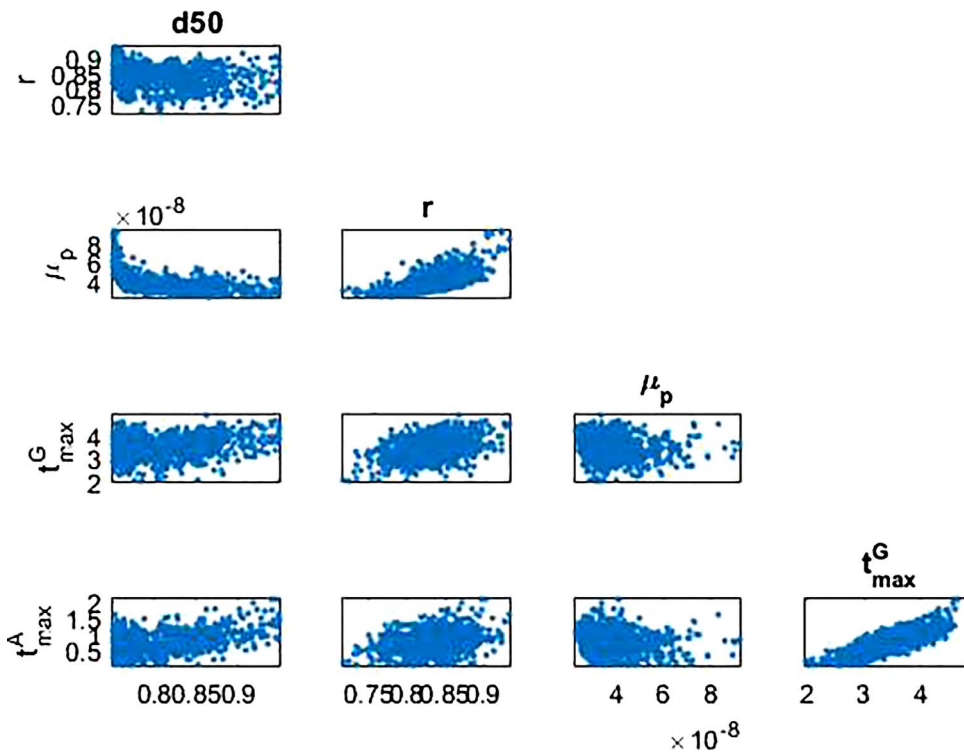


Fig. 8. Pairwise distributions of parameters for Version 1 for LLIN treated with an IconMaxx LN kit.

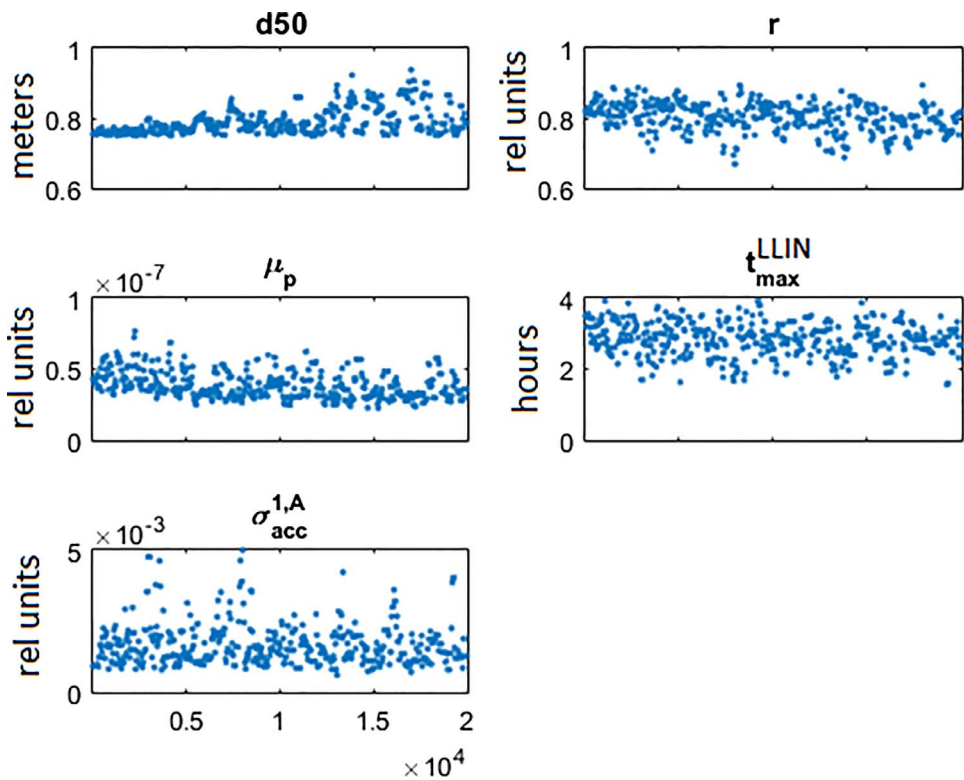


Fig. 9. Parameter chains for Version 2 for LLIN treated with an IconMaxx LN kit.

Different model versions were also tested in community-scale simulations. It appears that the calibrated model can be used to estimate the overall impact of the LLINs, in spite of the fact that the underlying parameters are not uniquely identified: key factors such as the mosquito mortality and mosquito-human contact rate under various degrees of protection remain essentially the same even when simulated using different parameter values from the sampled MCMC posteriors.

Moreover, the community-scale simulation indicated the reduced efficiency of the LLINs in controlling of the *An. arabiensis* in comparison to *An. gambia*, regardless of the underlying modeling assumptions. It was concluded although the present work focuses on calibrating hut level data, the model can be applied to simulate the impact of LLINs for different settlement patterns.

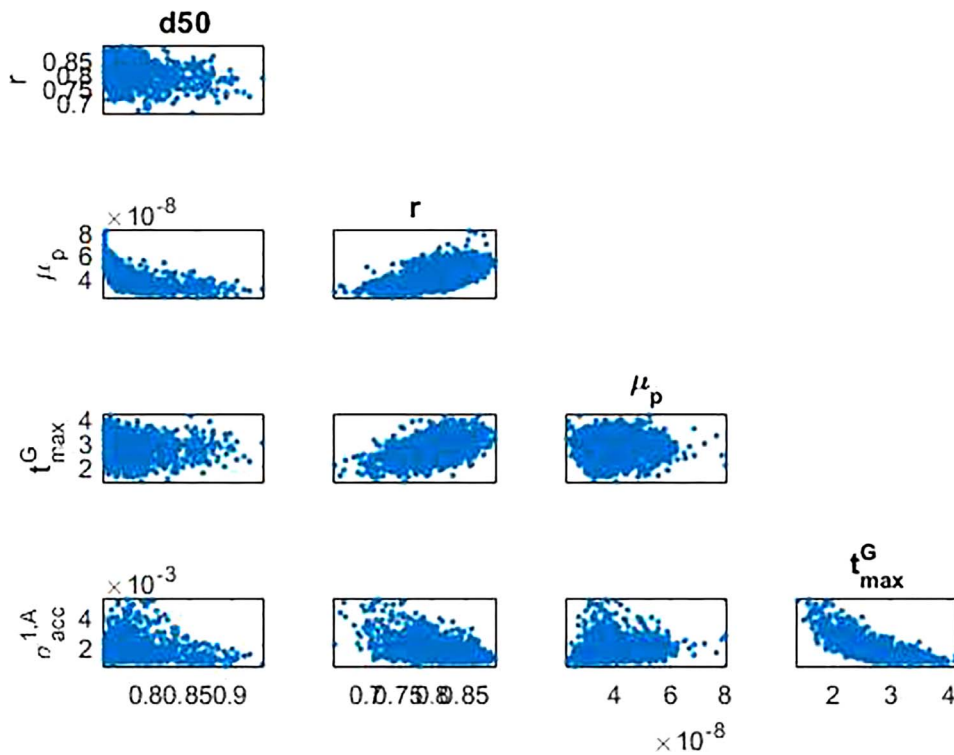


Fig. 10. Pairwise distributions of parameters Version 2 for LLIN treated with an IconMaxx LN kit.

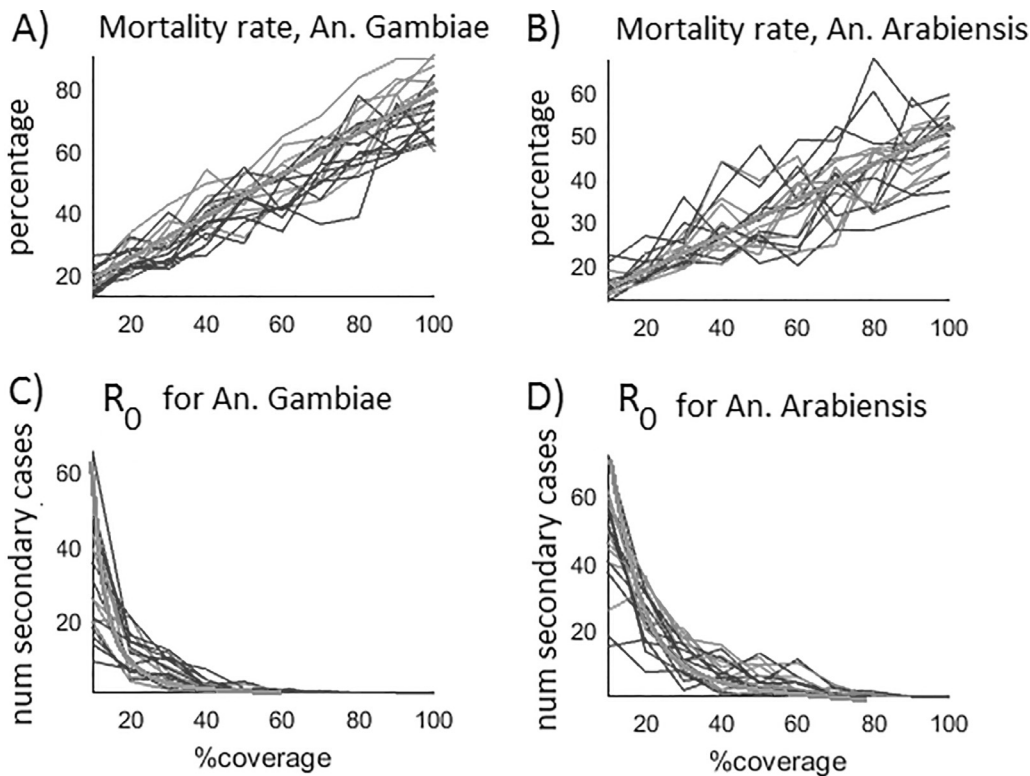


Fig. 11. Mortality rate and reproduction number R_0 conditioned on LLIN coverage for *An. gambiae* (left) and *An. arabiensis* (right) simulated using two different modifications of the model: Version 1 (blue line) and Version 2 (red line). (For interpretation of the references to colour in this figure legend, the reader is referred to the web version of this article.)

Acknowledgments

The research leading to these results was partly supported by funding from the European Union Seventh Framework Programme (FP7/2007-2013 grant agreement 265660), AvecNet and by the Center of Excellence in Inverse Problems of the Academy of Finland [grant number 284715].

References

- [1] S. Almeida, R. Ferreira, R. Eiras, R. Obermayr, M. Geier, Multi-agent modeling and simulation of an *aedes aegypti* mosquito population, *Environ. Model Softw.* 25 (12) (2010) 1490–1507.
- [2] M. Bowen, The sensory physiology of host-seeking behavior in mosquitoes. *Annu. Rev. Entomol.* 36 (1991) 139–158.
- [3] R. Cardé, Odour plumes and odour-mediate flight in insects, *Ciba. Found. Symp.* 200 (1996) 54–66.

- [4] D. Chao, S. Halstead, M. Halloran, I. Longini, Controlling dengue with vaccines in thailand, *PLoS Negl. Trop. Dis.* 6 (10) (2012) e1876.
- [5] A. Clements, G. Paterson, The analysis of mortality and survival rates in wild populations of mosquitoes, *J. Appl. Ecol.* 18 (1981) 373–399.
- [6] B. Cummins, R. Cortez, I. Foppa, J. Walbeck, J. Hyman, A spatial model of mosquito host-seeking behavior, *PLoS Comput. Biol.* 8 (5) (2012) e1002500.
- [7] K. Dale, T. Collett, Using artificial evolution and selection to model insect navigation, *Curr. Biol.* 11 (17) (2001) 1305–1316.
- [8] T. Dekker, R. Cardé, Moment-to-moment flight manoeuvres of the female yellow fever mosquito (*aedes aegypti* L.) in response to plumes of carbon dioxide and human skin odour, *J. Exp. Biol.* 214 (20) (2011) 3480–3494.
- [9] T. Dekker, M. Geier, R. Cardé, Carbon dioxide instantly sensitizes female yellow fever mosquitoes to human skin odours, *J. Exp. Biol.* 208 (2005) 2963–2972.
- [10] P. Eckhoff, A malaria transmission-directed model of mosquito life cycle and ecology, *Malar J.* 10 (2011) 1–17.
- [11] M. Gillies, Age-groups and the biting cycle in *Anopheles gambiae*. A preliminary investigation, *Bull. Entomol. Res.* 48 (03) (1957) 553–559.
- [12] M. Gillies, T. Wilkes, A comparison of the range of attraction of animal baits and of carbon dioxide for some west african mosquitoes, *Bull. Entomol. Res.* 59 (3) (1968) 441–456.
- [13] W. Gu, R. Novak, Agent-based modelling of mosquito foraging behaviour for malaria control, *Trans. R. Soc. Trop. Med. Hyg.* 103 (11) (2009) 1105–1112.
- [14] H. Haario, M. Laine, A. Mira, E. Saksman, Dram: efficient adaptive mcmc, *Comput. Stat.* 16 (2006) 339–354.
- [15] H. Haario, E. Saksman, J. Tamminen, Adaptive proposal distribution for random walk metropolis algorithm, *Comput. Stat.* 14 (3) (1999) 375–395.
- [16] H. Haario, E. Saksman, J. Tamminen, An adaptive metropolis algorithm, *Bernoulli* 7 (2) (2001) 223–242.
- [17] P. Kareiva, N. Shigesada, Analyzing insect movement as a correlated random walk, *Oecol* 56 (1983) 234–238.
- [18] H. Kawada, K. Ohashi, G. Dida, G. Sonye, S. Njenga, C. Mwandawiro, N. Minakawa, Preventive effect of permethrin-impregnated long-lasting insecticidal nets on the blood feeding of three major pyrethroid-resistant malaria vectors in western kenya, *Parasit Vectors* 7 (2014) 383.
- [19] G. Killeen, N. Chitnis, S. Moore, F. Okumu, Target product profile choices for intradomestic malaria vector control pesticide products: repel or kill? *Malar J* 10 (2011) 207.
- [20] S. Kirkpatrick, C. Gelatt, M. Vecchi, Optimization by simulated annealing, *Science* 220 (4598) (1983) 671–680.
- [21] J. Kitau, R. Oxborough, P. Tungu, J. Matowo, R. Malima, S. Magesa, J. Bruce, F. Moshia, M. Rowland, Species shifts in the *Anopheles gambiae* complex: do llins successfully control *Anopheles arabiensis*? *PLoS ONE* 7 (3) (2012) e31481.
- [22] M. Lehane, *The Biology of Blood-Sucking in Insects*, Second Edition. second ed, Cambridge University Press, NY, 2005.
- [23] L. Lorenz, A. Keane, J. Moore, C. Munk, L. Seeholzer, A. Mseka, E. Simfukwe, J. Ligamba, E. Turner, L. Biswaro, F. Okumu, G. Killeen, W. Mukabana, S. Moore, Taxis assays measure directional movement of mosquitoes to olfactory cues, *Parasit Vectors* 6 (2013) 131.
- [24] C. Manore, K. Hickmann, J. Hyman, I. Foppa, J. Davis, D. Wesson, C. Mores, A network-patch methodology for adapting agent-based models for directly transmitted disease to mosquito-borne disease, *J. Biol. Dyn.* 9 (1) (2015) 52–72.
- [25] N. Metropolis, A. Rosenbluth, M. Rosenbluth, A. Teller, E. Teller, Equations of state calculations by fast computing machines, *J. Chem. Phys.* 21 (6) (1953) 1087–1092.
- [26] F. Okumu, E. Mbeyela, G. Lingamba, J. Moore, A.J. Ntamatungiro, D. Kavishe, K. M.G., L. Turner E. and Lorenz, S. Moore, Comparative field evaluation of combinations of long-lasting insecticide treated nets and indoor residual spraying, relative to either method alone, for malaria prevention in an area where the main vector is *Anopheles arabiensis*, *Parasit Vectors* 6 (2013) 46.
- [27] H. Padmanabha, F. Durham David orrea, M. Diuk-Wasser, A. Galvani, The interactive roles of *Aedes aegypti* super-production and human density in dengue transmission, *PLoS Negl. Trop. Dis.* 6 (8) (2012) e1799.
- [28] M. Reddy, H. Overgaard, S. Abaga, V. Reddy, A. Caccone, A. Kiszewski, M. Slotman, Outdoor host seeking behaviour of *Anopheles gambiae* mosquitoes following initiation of malaria vector control on bioko island, equatorial guinea, *Malaria J.* 10 (184) (2011).
- [29] K. Senda, T. Obara, M. Kitamura, N. Yokoyama, N. Hirai, M. Lima, Aerodynamic forces and vortical structures in flapping butterfly's forward flight, *Phys. Fluids* 7 (2) (2012) 025002.
- [30] N. Shimizu, C. Ogino, T. Kawanishi, Y. Hayashi, Fractal analysis of daphnia motion for acute toxicity bioassay, *Environ. Toxicol.* 17 (2) (2002) 441–448.
- [31] D. Smith, F. McKenzie, R. Snow, S. Hay, Revisiting the basic reproductive number for malaria and its implications for malaria control, *PLoS Biol.* 5 (3) (2007).
- [32] W. Snow, Field estimates of the flight speed of some west african mosquitoes, *Ann. Trop. Med. Parasitol.* 74 (2) (1980) 239–242.
- [33] J. Spitzen, C. Spoor, F. Gieco, C. Braak, J. Beeuwkes, S. van Brugge, S. Kranenbarg, L. Noldus, J. van Leeuwen, W. Takken, A 3d analysis of flight behavior of *Anopheles gambiae* sensu stricto malaria mosquito in response to human odor and heat, *PLoS ONE* 8 (5) (2013) e62995.
- [34] Z. Syed, W. Leal, Acute olfactory response of *Culex* mosquitoes to a human and bird-derived attractant, *Proc. Natl. Acad. Sci. U S A* 106 (44) (2009) 18803–18808.
- [35] I. van den Broek, C. den Otter, Olfactory sensitivities of mosquitoes with different host preferences (*Anopheles gambiae* s.s., *an. arabiensis*, *an. quadriannulatus*, *an. m. atroparvus*) to synthetic host odours, *J. Insect. Physiol.* 45 (11) (1999) 1001–1010.
- [36] J. Vaughan, B. Noden, J. Beier, Concentrations of human erythrocytes by *Anopheline* mosquitoes (*Diptera: Culicidae*) during feeding, *J. Med. Entomol.* 28 (6) (1991) 780–786.
- [37] N. Vickers, Mechanisms of animal navigation in odor plumes, *Biol. Bull.* 198 (2) (2000) 203–212.
- [38] WHO, Guidelines for testing mosquito adulticides for indoor residual spraying and treatment of mosquito nets, Technical Report, Geneva: WHO, 2006.